Correction to the last part of p. 4 in the Specific comments

In the answer to the referee 1, there was a mistake: previously forested areas were taken into account in the calculations of NDVI distributions. We have performed new calculations only for dry tundra sites (according to the topographic map). The areas of the sites used for calculations and the percentages of forested areas calculated from NDVI analysis have changed but the main conclusions remained the same. Please find the corrected version below.

> *Fig 8 – what is displayed here exactly? This remains unclear based on the corresponding methods section and figure title. Is the standard deviation based on spatial variation for the background sites? How is temporal variation in NDVI of the background sites accounted for? Are the different years and the background areas statistically balanced for their size?*

In the previous version of the manuscript, Fig. 8a showed the distribution of NDVI over study area 1 based on the Landsat data from 3 July 2019. The curves of different colors indicated boundaries of the background tundra sites and burned tundra sites detected in the Landsat mosaics from different years (see legend). Fig. 8b showed mean NDVI indices and standard deviations calculated for the background areas and the areas burned in different years as indicated in panel (a). The standard deviation was based on the spatial variation of NDVI (determined by the number of pixels with different NDVI within each area) and temporal dynamics was not accounted for. Instead of mean values and standard deviations, in the current version of the manuscript we use distributions of NDVI and extend NDVI-related analysis (sec. 3.3.1). We also show NDVI based on Landsat data from 30 June 2018 instead of data from 3 July 2019 for the reason described below. Therefore, Fig. 8 has changed (see Fig. 2 in this document).
In order to make the areas more balanced by size, we merged the data sets for 1968 and 1988, for which we might expect that vegetation has recovered after fires, based on the mean NDVI values. As a result, all study areas were larger than 600 km^2 (1968+1988 – 600 (405+195) km^2, 2001 – 1565 km^2, 2018 – 867 km^2, background – 937 km^2). (*Lines 193-195*)

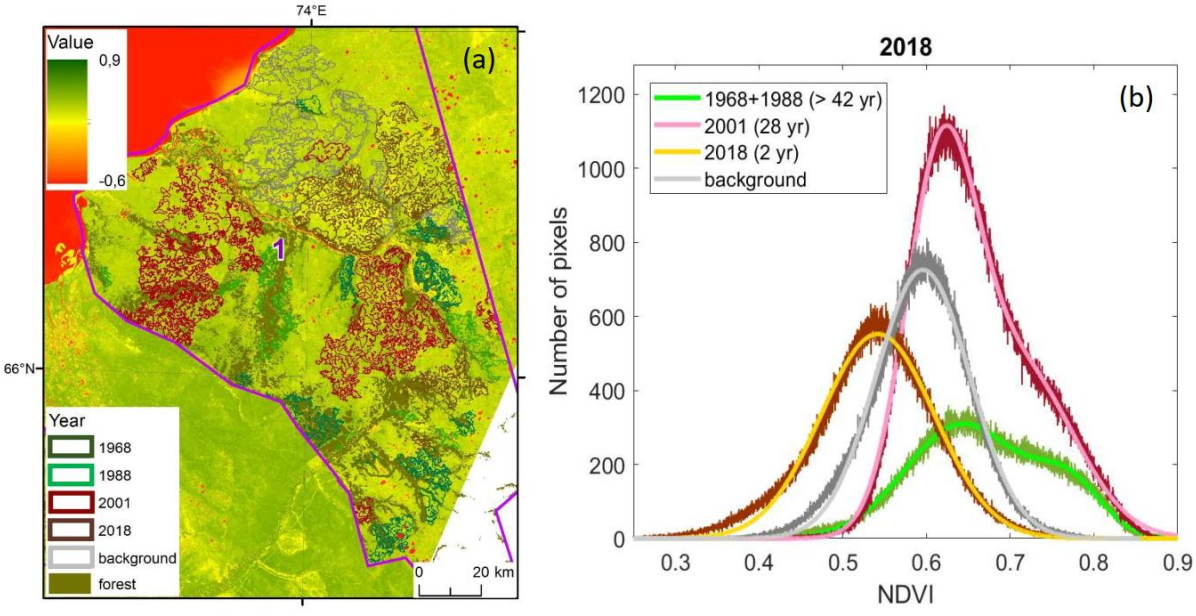

Fig. 2. (a) The distribution of NDVI over study area 1 on 30 June 2018. Segments with boundaries of different color are background dry tundra sites and burned dry tundra sites detected in the Corona and Landsat mosaics from different years (see legend). Burned areas in the mosaics from 1968 and 1988 are mainly due to fires from >42 years ago, in 2001 – due to fires from 28 years ago, in 2018 – due to fires from

2 years ago. (b) Distributions of NDVI based on the data from background sites and the sites burned in different years. In the legend, numbers in brackets indicate years after the last major fire.

Fig. 2b (Fig. 8b in the new version of the manuscript) shows the distributions of NDVI for the burned areas detected in 1968+1988, 2001, 2018, and for background areas. Using the dates of major fires and the date of Landsat mosaic (2018), we can assume that NDVI within burned tundra sites detected in 1968 and 1988 reflect the state of vegetation after fires more than 42 years ago, in 2001 – after fires 28 years ago, in 2018 – after fires 2 years ago. NDVI in background tundra refers to tundra not affected by fires during the whole study period.

The distributions from the background tundra and recently burned sites are close to Gaussian ones. Interestingly, the distributions from the sites burned 28 and >42 years ago are bimodal and they have higher NDVI values as compared to the background and recently burned sites. We fitted the bimodal distributions by the sums of two Gaussian functions and determined mean values and standard deviations for all the peaks (Table 1 in this document, Table 7 in the new version of manuscript). The positions of the lower peaks of the bimodal distributions differ only slightly, whereas the position of the upper peak is a bit lower and the peak is less pronounced for the area burned 28 years ago.

Further, we used the mean values and standard deviations to identify vegetation associated with the peaks of the distributions in the satellite images. For illustration, we chose an image containing all representative examples of vegetation (Fig. 3 in this document, Fig. 9 in the new version of manuscript).

Green color in Fig 3, right panel, indicates the pixels which have NDVI in the interval ($NDVI_{max,2}$-σ_2; $NDVI_{max,2}$+σ_2) corresponding to the upper peak of the distribution based on the data from 1968+1988. Comparing left panel and right panel of Fig. 3, one can conclude that this peak is mainly associated with forests. The lower peak (pixels in blue color in Fig. 3, right panel), as can be seen from Fig. 3, corresponds to woodlands and tundra. This lower peak has a large intersection with the peak in the unimodal distribution from the background site (Fig. 2b). However, interestingly, there is a significant decrease in the pixels with NDVI below ca 0.52 in the bimodal distributions. These pixels are marked in pink in Fig. 3, right panel. They correspond to the tundra sites lightest in color due to the presence of lichen in the vegetation community. The fraction of such pixels decreases in bimodal distributions, meaning that lichen does not recover to its state before the fire. Instead, bimodal distributions gain a large fraction of pixels with high NDVI corresponding to forests.

Table 1. Parameters of fits of the NDVI distributions in Fig. 2b by Gaussian functions

$$N_{pix} = A_1 \exp\left(-\frac{(NDVI-NDVI_{max,1})^2}{2\sigma_1^2}\right) + A_2 \exp\left(-\frac{(NDVI-NDVI_{max,2})^2}{2\sigma_2^2}\right).$$

Year	A_1	$NDVI_{max1}$	σ_1	A_2	$NDVI_{max2}$	σ_{max2}
1968+1988	308	0.64	0.07	132	0.77	0.04
2001	954	0.62	0.04	448	0.71	0.06
2018	552	0.54	0.07	-	-	-
Background	726	0.59	0.06	-	-	-

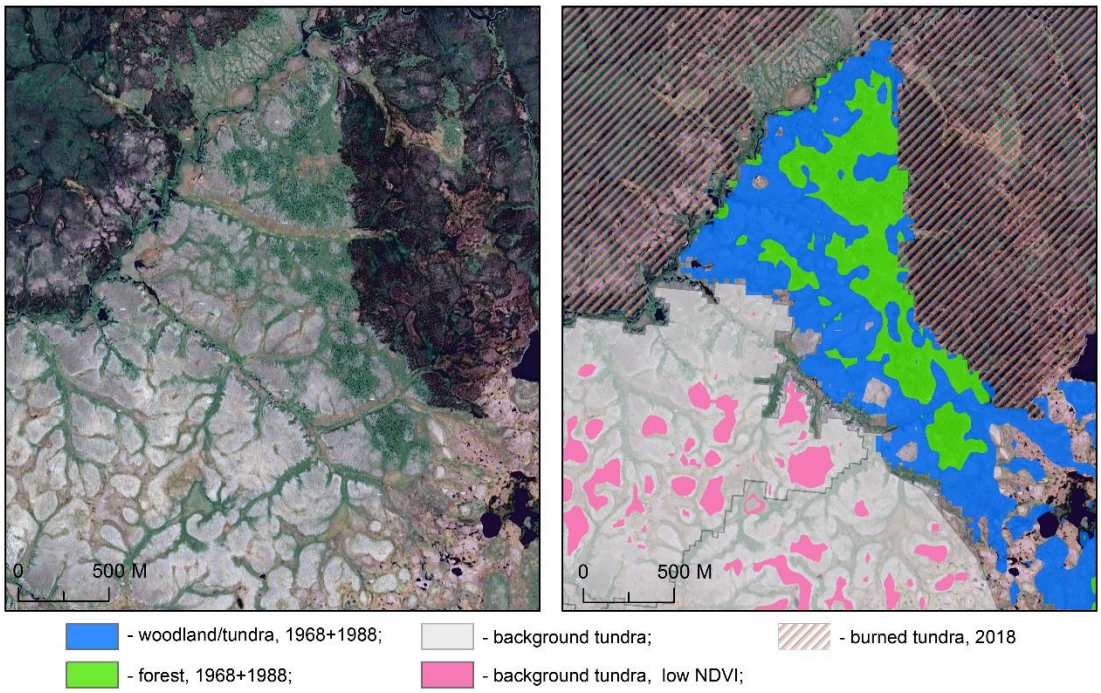

Fig. 3. Representative types of vegetation associated with different state of the sites and NDVI. Left panel: an image without mask, right panel: the same image colored according to the state of the site (burned in mosaics from 1968+1988 or 2018, background) and NDVI. In the right panel, green color corresponds to the upper peak and blue color corresponds to the lower peak in the bimodal distribution from the sites burned before 1968/1988 (Fig. 2b). Pink color marks pixels with NDVI lower than 0.52 in the background site.

We compared NDVI distributions based on Landsat 8 data from 30 June 2018 and 03 July 2019 (Fig. 4 in the current document). These dates were chosen close to the peak of daily temperature and should be representative of the peak growing season. The distributions of NDVI are largely similar for both years. However, for NDVI based on mosaic from 2019, the upper peak in the bimodal distributions is less pronounced (in 2001-distribution it looks more like asymmetry) and there appears a lower peak in the distribution corresponding to recent fires. This could be due to different phenological state of vegetation, dependent on temperature and precipitation from year to year. The peak corresponding to tundra vegetation and woodlands almost did not change its position in both figures, but the peak of the distribution after the recent fire (2018 in the legends) and 'forest' peaks in bimodal distributions have larger NDVI in 2018.

Finally, we estimated the fraction of 'forest' pixels in the bimodal distributions. We used NDVI data from 2018, as the separate peaks were better pronounced in bimodal distributions. Using standard deviations of the two peaks, the boundary approximately separating forest peak from tundra peak corresponds to the threshold value of NDVI=0.72. We assume that pixels with NDVI > 0.72 represent mainly forest, and pixels with NDVI<0.72 – tundra and woodlands. We integrated the distribution to find the fraction of pixels with NDVI>0.72 in the total number of pixels. In the areas burned 28 years ago, forests occupied 19% of the total area. In the areas burned more than 42 years ago, the forest fraction increased to 28% of the total area. This number is comparable to our estimates of the vegetation shift within the forest-tundra and northern taiga zone (14-56%).

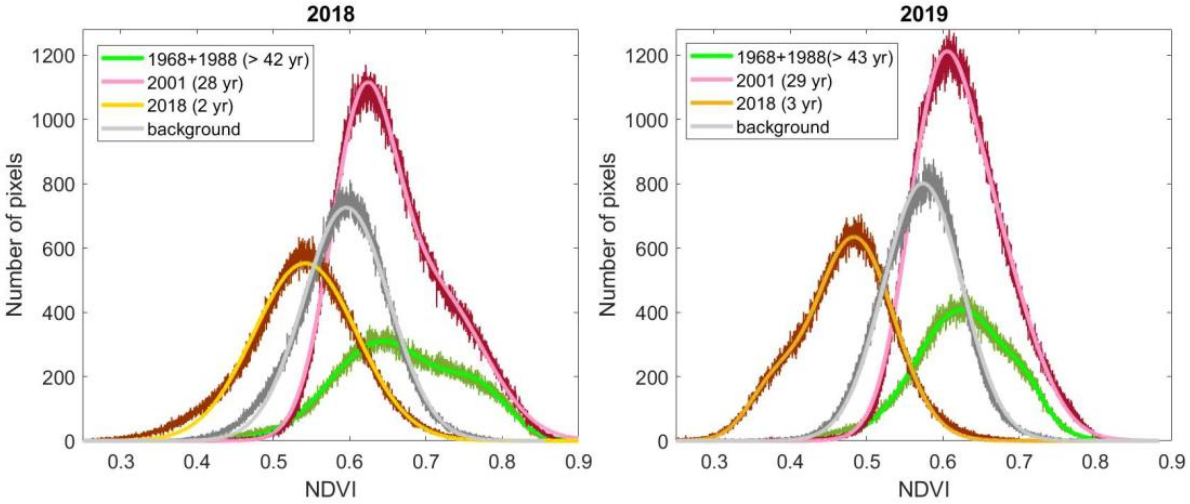

Fig. 4. Distributions of NDVI in the burned and background dry tundra areas based on the images from 30 June 2018 (left panel) and 3 July 2019 (right panel). In the legend, years correspond to these of mosaics used to calculate burned territories, numbers in brackets indicate years after last major fire.

While precise estimates of forest fraction based on NDVI are challenging, the main results following from Figs. 2 and 3 can be summarized as follows:

1. The NDVI distributions based on the data from background tundra and areas burned 2 years ago are predominantly unimodal, whereas the distributions based on the data from areas burned 28 years ago and earlier are bimodal.
2. The low-NDVI pixels corresponding to vegetation communities in tundra characterized by relatively high amounts of lichen and thus having lightest colors in the images largely disappear from the distributions corresponding to vegetation communities recovered after fires.
3. Instead, the new state of vegetation recovered after fires is characterized by a higher mean NDVI due to the new peak associated with forest. The fraction of pixels representing forest increases with time after the last fire.